引用格式：WANG Xiao-fa，LIU Jing-hui，JIN Zeng-gao. State-switchable Multi-wavelength and Dissipative Soliton Mode-locked Tm-doped Fiber Laser Based on a Combination of Nonlinear Amplifying Loop Mirror and Lyot Filter[J]. *Acta Photonica Sinica*，2020，**49**(4)：0414001

王小发，刘经惠，靳增高. 基于非线性放大环镜和 Lyot 滤波器的多波长与耗散孤子锁模态开关型掺铥光纤激光器[J]. 光子学报，2020，**49**(4)：0414001

基于非线性放大环镜和 Lyot 滤波器的多波长与耗散孤子锁模态开关型掺铥光纤激光器

王小发，刘经惠，靳增高

（重庆邮电大学 光电工程学院，重庆光纤通信技术重点实验室，重庆 400065）

摘　要：报道了一种基于非线性放大环镜和 Lyot 滤波器技术的态开关型掺铥光纤激光器. 通过仔细调节偏振控制器和泵浦功率，掺铥光纤激光器可以分别在多波长态和耗散孤子锁模态运行，并且两种态之间可以相互切换. 对于多波长态，在光谱半功率值范围内能生成 8 个稳定的波长；对于耗散孤子锁模态，在 1 996 nm 的中心波长处产生脉冲能量高达 41.49 nJ，脉冲持续时间为 2.4 ns，光谱带宽为 29 nm 的耗散孤子. 不同运行态间的切换归因于偏振控制器导致的非线性放大环镜的功能的改变.

关键词：非线性放大环镜；Lyot 滤波器；多波长；耗散孤子；光纤激光器

中图分类号：TN248　　**文献标识码**：A　　**doi**：10.3788/gzxb20204904.0414001

State-switchable Multi-wavelength and Dissipative Soliton Mode-locked Tm-doped Fiber Laser Based on a Combination of Nonlinear Amplifying Loop Mirror and Lyot Filter

WANG Xiao-fa，LIU Jing-hui，JIN Zeng-gao

（*Key Laboratory of Optical Fiber Communication Technology*，*College of Optoelectronic Engineering*，*Chongqing University of Post and Telecommunications*，*Chongqing* 400065，*China*）

Abstract：This paper demonstrates a state-switchable Tm-doped fiber laser based on nonlinear amplifying loop mirror and Lyot filter technique. By properly adjusting the polarization controller and pump power，the Tm-doped fiber laser can operate in multi-wavelength state and dissipative soliton mode-locked state，respectively. And two types of operating states can be switched to each other. For multi-wavelength state，8 stable wavelength peaks are generated within half of peak power variation. For the dissipative soliton mode-locked state，the dissipative soliton with pulse energy as high as 41.49 nJ，the pulse duration of 2.4 ns，and the spectrum bandwidth of 29 nm is generated at the center wavelength of 1 996 nm. The switching between different operating states is due to the change in the function of the nonlinear amplifying loop mirror caused by the polarization controller.

Key words：Nonlinear amplifying loop mirror；Lyot filter；Multi-wavelength；Dissipative soliton；Fiber laser

OCIS Codes：140.4050；140.3538；190.4370；060.3510

Foundation item：National Natural Science Foundation of China（No. 11304409），Nature Science Foundation of Chongqing（No. cstc2018jcyjA0655），Science and Technology Commission Project of Chongqing（No.cstc2017zdcy-zdzxX0011）

First author：WANG Xiao-fa（1978－），male，associate professor，Ph.D. degree，mainly focuses on solid-state laser and fiber laser technology. Email：wangxf@cqupt.edu.cn

Received：Nov.12，2019；**Accepted**：Jan.7，2020

0 Introduction

In recent years, 2 μm fiber laser with the advantage of operating at the atmospheric window and eye-safe wavelength range[1-2] has developed rapidly due to its wide range of applications in laser space communication, laser biomedical treatment and laser sensing fields[3-5]. 2 μm fiber laser with different operating states is required in different fields. For example, Multi-Wavelength (MW) fiber laser plays an important part in the fields of Wavelength Division Multiplexing (WDM) systems, sensing systems and microwave photonics[6-8]. At present, most of researches about MW fiber laser focus on the 1.5 μm region[6-7, 9-10] at home and abroad. In contrast, there have been fewer works on MW fiber laser at 2 μm wavelength region[11-18]. The common methods for realizing the MW laser are to combine the periodic response characteristics of a comb filter, such as Mach-Zehnder Interferometer (MZI)[10], tapered fiber[3, 6], Lyot filter[2, 12], Sagnac loop[13-14], with the gain characteristics of a doped fiber[3]. Wang, *et al*. obtained single-wavelength, dual-wavelength, and three-wavelength Tm-doped fiber laser based on a micro fiber-optic Fabry-Perot Interferometer (FPI) and a Nonlinear Optical Loop Mirror (NOLM)[6]. Liu, *et al*. implemented multi-wavelength fiber laser based on Nonlinear Polarization Rotation (NPR) and Lyot filter[12]. The adjustment of the wavelength interval can be achieved by changing the length of the polarization-maintaining fiber. Peng, *et al*. realized a 1.97 μm multiwavelength Tm-doped fiber laser based on a Nonlinear Amplification Loop Mirror (NALM) and a polarization-maintaining fiber loop mirror[13]. Yan, *et al*. implemented a tunable multi-wavelength mode-locked Tm-doped fiber laser based on NPR technology with birefringent fiber[15]. In addition, utilizing some mechanisms and effects used to suppress spectrum broadening can also achieve stable MW state. These include Four-Wave Mixing (FWM)[16], Stimulated Brillouin Scattering (SBS)[17].

On the other hand, high-energy ultrafast mode-locked fiber laser operating at 2 μm region plays important role in optical communication, material processing and laser medical treatment. But there still exist some problems for obtaining high energy pulse. Since the high anomalous dispersion of TDF and single-mode fiber in 2 μm region, the mode-locked pulse is usually limited to conventional soliton pulse. As the result of soliton area theory[19], the energy of conventional soliton pulse is usually no more than 0.1 nJ and the spectrum width is usually only a few nanometers[20-21]. So far, various high energy pulses have been developed continually by different technologies, such as dispersion management soliton[4, 22], self-similar soliton[23], noise-like pulse[24-25], Dissipative Soliton (DS)[26-28]. By contrast, the DS is considered as a better choice, which can tolerate by three orders of magnitude higher energy than others. The DS pulse can be generated by using some mode-locked mechanisms, such as NPR[4, 29-31], NOLM[19], NALM[32-34], Carbon Nanotube (CNT)[21-22], Semiconductor Saturable Absorber Mirror (SESAM)[35-36], molybdenum disulfide (MoS_2)[37]. Compared with other methods, NALM as an artificial saturable absorber has the advantages of higher damage threshold, low cost and all-fiberization[38-39], which is a better way to achieve high energy DS pulse.

To date, the fiber laser with switchable operating states has become the focus of researches and has been reported in related literatures. Recently, a switchable soliton mode-locked and MW fiber laser has been reported based on the NPR technique[11]. And Yun, *et al*. demonstrated a switchable vector dissipative soliton and conventional soliton fiber laser based on the CNT saturable absorber and the Lyot filter[21]. As far as we know, for NPR technique[11], due to the inherent characteristics of polarization-dependent isolator, large insertion loss is caused. And polarization dependent isolator is expensive. And the CNT saturable absorber of sandwich structure has low thermal damage threshold. Thus, it is necessary to study a kind of high damage threshold, low-cost, state-switchable fiber lasers. Up to now, the state-switchable MW and Dissipative Soliton Mode-Locked (DSML) Tm-Doped Fiber Laser (TDFL) has not been reported based on the NALM and Lyot filter.

In this paper, we demonstrate a state-switchable TDFL based on NALM with a Lyot filter, delivering two types of operating states: MW and DSML. The two types of states can be switched by carefully adjusting Polarization Controller (PC). When NALM acts as an amplitude equalizer, the MW state with uniform wavelength spacing can be obtained. In the case of NALM acts as a saturable absorber, the stable

DSML state can be realized. We also further investigated the switching of MW state and DSML state. This work lays a foundation for further study of the nonlinear dynamic characteristics of the fiber lasers.

1 Experimental setup and principle

The experimental setup of the state-switchable TDFL in a figure-eight configuration is illustrated in Fig.1. The cavity consists of two fiber loops, unidirectional ring (left) and NALM (right), which are connected to each other by a 50∶50 Optical Coupler (OC). In the NALM, a 4.5 m double clad Tm-doped fiber (TDF, IXF-2CF-Tm-O-10-130, IX Fiber) with core/inner-cladding diameter of 10/125 μm is used as the gain medium. Its absorption coefficient is 5.6 dB/m at 789 nm. The fiber laser is pumped by a semiconductor multimode fiber laser with maximum power of 12 W operating at 793 nm via a (2+1) ×1 signal-pump combiner. A 6 m SMF-1950 single-mode fiber dedicated to 2 μm band is used to enhance the nonlinearity in the cavity. A Lyot filter consisted of PC and a piece of 5.8 m Polarization Maintain Fiber (PMF) with beat length and birefringence of 5.2 mm at 1 950 nm and nominal 3.5×10^{-4}, respectively. In unidirectional ring, the isolator is used to ensure the unidirectional transmission. The 30% port of the OC with SMF-1950 pigtail fiber is used as the output port of the fiber laser. The rest of the fiber is SMF-28e fiber. The total length of the cavity is approximately 29.5 m.

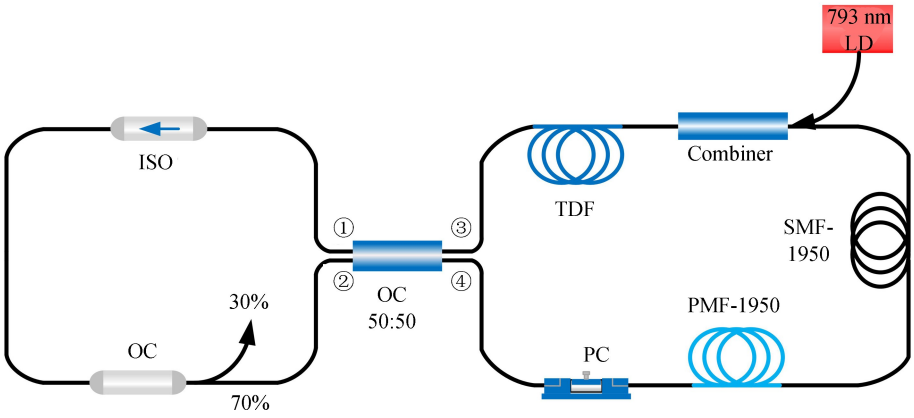

Fig.1 Schematic diagram of the experimental setup

The output characteristics of TDFL are measured by a power meter (7Z01560, OPHIR), a 1 GHz digital sampling oscilloscope (WaveRunner 610Zi, Lecroy) with an InGaAs photodetector (ET-5000F, EOT), an optical spectrum analyzer (Omni-λ 750i, Zuolix) with a resolution of 0.05 nm, and a spectrum analyzer (FSL3, Rohde&Schwarz) with 3 GHz bandwidth.

NALM is a key component for this experimental setup. The incident field from port 2 of the 3 dB coupler splits into two propagation fields with equal amplitudes and opposite directions. The two beams are transmitted in the TDF and the single-mode fiber, respectively. And a certain phase difference can be generated after a round trip. The two beams combine and interface in 3 dB coupler when they come back from port 3 and port 4. Then the reflected and transmitted filed emerge from port 2 and port 1 of the 3 dB coupler, respectively. The transmission of NALM can be simplified as the Eq. (1)[7, 9, 13]

$$T=\frac{P_{\mathrm{T}}}{P_{\mathrm{in}}}=G\{1-k\,[1+\cos\,(k(1-G)\gamma P_{\mathrm{in}}L+\theta)\,]\} \tag{1}$$

where, P_{T} is the transmissive power; P_{in} is the input power; G is the gain factor of the TDFA; k is the split ratio of the 3 dB coupler, and the value is 0.5; γ is the nonlinear coefficient of the SMF-1950 and PMF-1950, and the value is 2.0 $\mathrm{W^{-1}\cdot km^{-1}}$; L is the total length of SMF-1950 and PMF-1950, the value is 11.8 m; θ is the phase bias caused by PC. With a given G factor, variation characteristics of transmission curve can be shifted by altering θ. As the result that the function of NALM can be switched by adjusting the PC. As θ is the certain value set by PC, the slope of the transmittance curve is positive, as shown by the solid line in Fig.2. The low-intensity continuous wave light and the leading and trailing edges of the pulse have a gain smaller than that of the high-intensity pulse center. After multiple round trips, a stable mode-locked pulse is formed, so that NALM acts as a saturable absorber. In contrast, by adjusting θ to

make the slope of the transmittance curve negative, as shown by the dashed line in Fig. 2, the gain of low-intensity light is greater than the gain of high-intensity light. Therefore, NALM acts as an amplitude equalizer which can suppress mode competition for multi-wavelength operation.

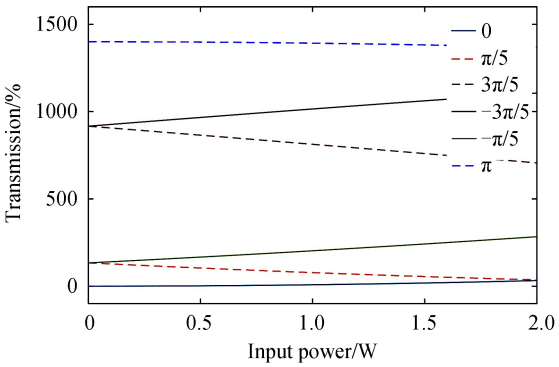

Fig.2 NALM transmission characteristics at different θ values with a given G

2 Experimental results and discussion

2.1 TDFL operating at MW state

When the pump power is increased to 3.7 W and proper phase bias is chosen via adjusting PC, the MW state is easily achieved. The output spectrum with 8 peaks wavelength is shown in Fig. 3(a). In the experiment, the Lyot filter working as a comb filter in the cavity is here a key component for generating MW laser[2, 12]. A piece of PMF introduced into the cavity of TDFL can increase the available channels[18]. The spacing between two adjacent channels is determined by the length of the birefringent fiber[12], the modal birefringence, and the center wavelength of the fiber laser, which can be given by the Eq. (2)

$$\Delta\lambda = \frac{\lambda^2}{\Delta n L} \tag{2}$$

in which L is the fiber length of PMF, Δn is the effective refractive index difference between the two orthogonal axes[2]. In the experiment, the experimental value of L is 5.8 m. The spacing between two adjacent channels is calculated by Eq. (2) to be approximately 1.94 nm, which can be seen by zooming in the modulated spectrum. Accordingly, the value of Δn could be calculated as 3.57×10^{-4} that is approximately consisted with the parameters of PMF. In Ref. [12], Lyot filter is used as wavelength selection component, and NPR is used as an amplitude equalizer to suppress mode competition[12]. Compared with Ref. [13], in order to realize the MW laser operation, a section of polarization maintaining fiber is added to the NALM, and the experimental device is more concise. As can be seen from Fig. 3(a), the MW spectrum of the experiment is significantly different from Ref. [6], which is the MW state of continuous wave. The oscilloscope trace of MW state reported in this paper is in pulse train with strong fluctuation[2], indicating that the wavelength channels are not all continuous components. It is the result of the combination of NALM mode-locking effect and the Lyot filter filtering effect.

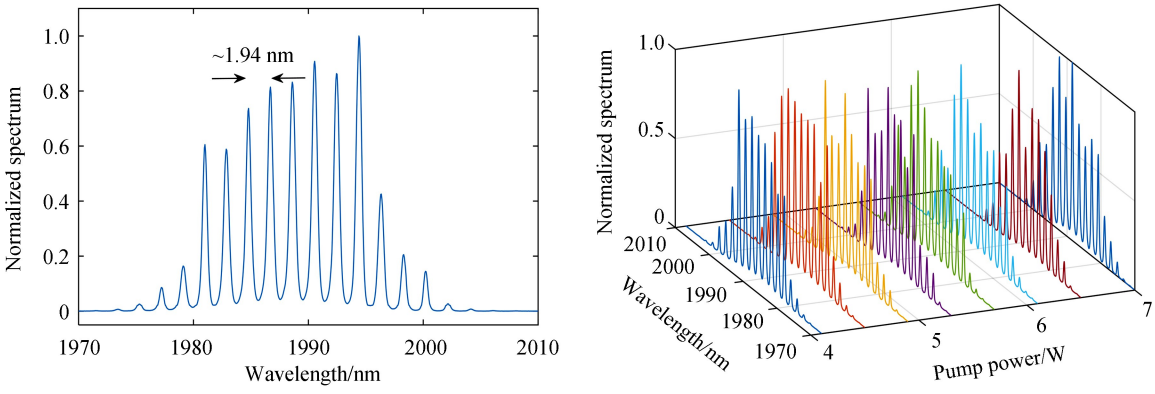

(a) Spectrum with 8 laser peaks (b) Evolution of spectrum with pump power

Fig.3 Experimental output characteristics of MW spectrum

Fig.3(b) shows the evolution of the wavelengthwith pump power while keeping PC state unchanged. Compared with Ref.[14] there is no significant change in the number of wavelengths as the pump power increased. It is worth noting that there is a fluctuation in the pulse wavelength as the result of inherent characteristics of the comb-induced filter of birefringence[3]. Rare-earth doped fiber with a wide range of laser radiation wavelengths provides the basis for MW output of fiber laser[1]. The double-clad TDF has a wide emission spectrum from 1.6 to 2.2 μm[1] and can withstand higher pump power, which provides a convenient operating environment for TDFL to achieve MW output. Because the wide non-flat gain curve of TDF, the gain values for different wavelengths are differential[14].

The experiment finds that the flatness of the multiple wavelengths is lowered with the increase of pump power. This may be due to the fact that the mode competition within the cavity is more intense, resulting in poor stability. It can be known from Eq.(1) that at higher pump power, the power scope served by the amplitude equalizer is reduced, which is not conducive to broadband MW oscillation[7]. Therefore, with the increase of pump power, the stability of MW system becomes worse.

Fig.4 shows the tunability of the MW state. By carefully adjusting the PC with the pump power unchanged, the tuning range of the MW spectrum is obtained between 1 970 nm and 2 020 nm, which is different from Ref.[8]. When NALM is used as an amplitude equalizer, a small adjustment of θ will not change the NALM state by fine-tuning the PC, but it will break the original gain and cavity loss to form a new balance, and changing the wavelength range of the laser[9]. The wavelength interval without change during the adjustment of PC. It can be known from Eq.(2), the wavelength channel spacing can be adjusted by changing the length of the PM fiber[12].

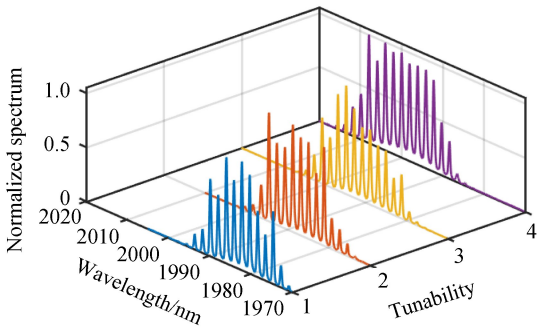

Fig.4 The tunability of MW state with different states of PC

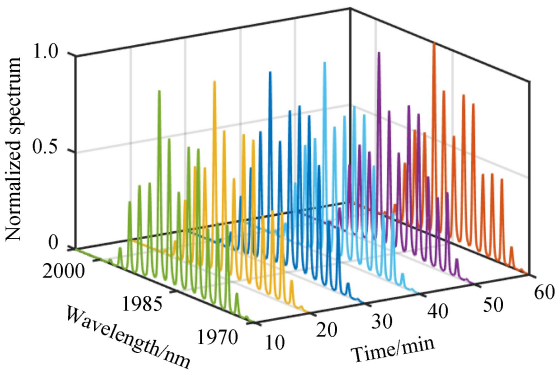

(a) Spectrum of MW state in an hour

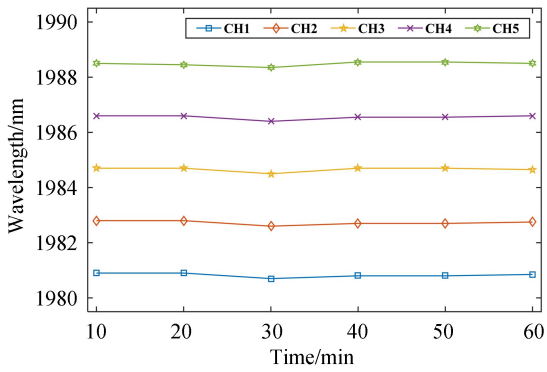

(b) Wavelength drifts of five channels in an hour

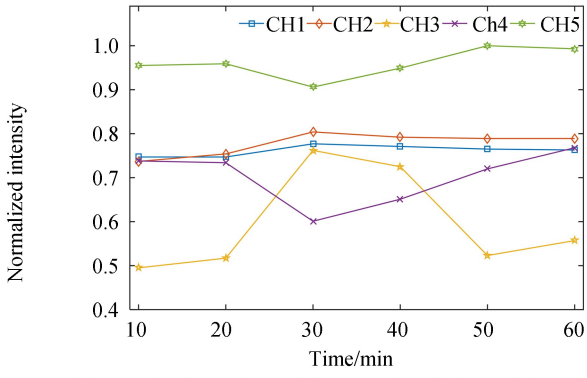

(c) Intensity fluctuations of five wavelength channels in an hour

Fig.5 Stability of MW state in an hour

In order to test the long-term stability of MW TDFL, MW spectrum is collected every 10 minutes in an hour with the pump power and the state of the PC unchanged. The results are shown in Fig.5. It can be seen from Fig.5(a), the distribution range of the spectrum has hardly changed. Fig.5(b) shows the change in the central wavelength of the five wavelength channels in the range from 1 980 nm to 1 990 nm. The result shows that the position of the spectrum channel changes less than 0.2 nm, indicating that the spectrum distribution range is relatively stable. Fig. 5 (c) shows the intensity fluctuations of five wavelength channels. The intensity fluctuations of channel 3 and channel 4 are larger than those of channel 1, channel 2 and channel 5. Fluctuations of wavelength channel intensity can be attributed to mode competition[12].

For MW fiber laser, TDF is a homogeneous broadening gain medium, which results in unfavorable mode competition. Since NALM is used as amplitude equalizer, small-intensity lasers gain more from NALM than high-intensity lasers. With the combined effect of Lyot filter, cavity gain and loss, stable MW laser oscillation can be formed[7]. For this experiment, it can be seen from the above experimental results, when the NALM acts as an amplitude equalizer, the distribution range of the MW spectrum is relatively stable, but the gain of some wavelength channels is not stable enough. It may be that the SMF-1950 in the device is relatively short[9]. At this time, the NALM-based amplitude equalizer does not work well in the suppression mode competition[8-9]. Therefore, the length of the SMF-1950 can be appropriately increased to improve the stability of the MW TDFL system.

2.2 TDFL operating at DSML state

In the case of NALM acts assaturable absorber by adjusting the PC, DSML state can be achieved at the pump power between 7.0 W and 10.5 W. The evolution of DSML state spectrum is shown in Fig.6(a), which is measured by an optical spectrum analyzer with bandwidth resolution of 0.05 nm from 1 965 nm to 2 035 nm. The measured Full Width at Half Maximum (FWHM) is approximately 29 nm at the center wavelength of 1 996 nm. The result shows that the spectrum shape is a bell shape[26] which is similar to relevant literatures about DS fiber laser at the 2 μm[36] and 1 μm[37]. But there is no steep edge and cat ear

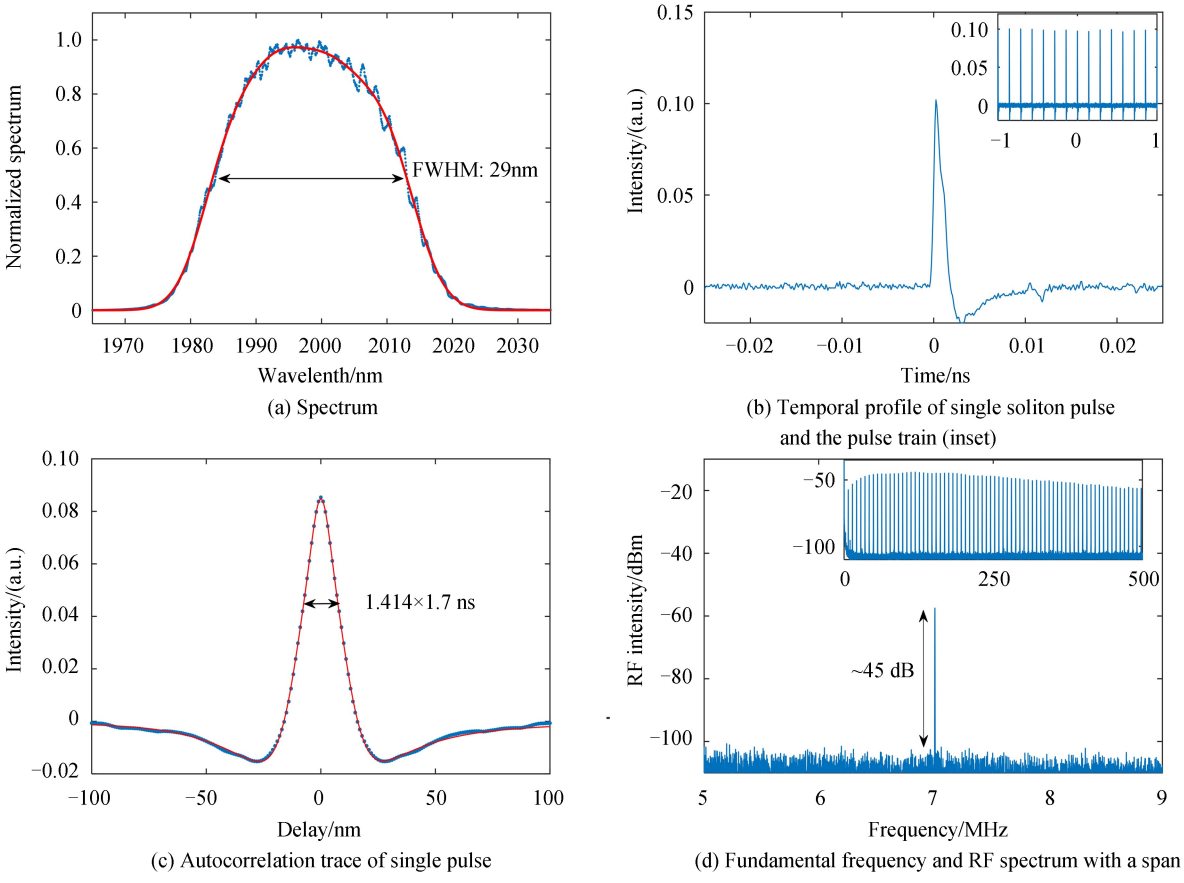

Fig.6 Experimental results of DSML state

sideband compared to the conventional DS spectrum[25, 30], which may be mainly due to the filtering effect of the Lyot filter[40].

The temporal profile of the singlesoliton and the soliton pulse train (inset) are illustrated in Fig. 6(b). The time profile of the DS soliton shows that the pulse has a steep edge at the front of the pulse, which clearly verifies the dissipative characteristic of the soliton[31]. The corresponding single pulse energy as high as 41.49 nJ is much larger than the single pulse energy of the traditional soliton mode-locked system. The soliton pulse has a sharply rising sharp front peak and a relatively slow changing trailing edge, which more clearly shows the h-like shape[41]. Another note worthy feature is that the trailing edge tow portion expands as the pump power increases. This phenomenon is similar to the case of dissipative soliton resonance. The flat trailing part of these time features is due to the peak-power-clamping effect[41]. According to the Refs. [26] and [38], the soliton pulse in this experiment is not completely forced and it is an excessive phenomenon of DS.

The autocorrelation trace of the pulse is presented in Fig. 6(c). The autocorrelation trace has a FWHM of approximately 2.4 ns. According to the Time Bandwidth Product (TBP) formula[21], the TBP of the DS pulse can be calculated up to 2181.5, indicating that the soliton pulse has a large chirp that is also a characteristic of DS. The formation of DS is a natural consequence of the mutual balance of cavity gain, loss, dispersion and nonlinearity[37]. Especially in dissipative system, the balance of gains and losses plays a crucial role[29].

In order to evaluate the stability of the DSML state, the RF spectrum of TDFL is measured by using a 1 kHz resolution RF spectrum analyzer. The results are presented in Fig. 6(d). The fundamental frequency and Signal-to-Noise Ratio (SNR) of the DS pulse are approximately 7 MHz and 45 dB, respectively. In addition, the inset RF spectrum with a scan range of 500 MHz shows that there are no other frequency components except the fundamental and harmonic frequencies. Meanwhile, it can be seen from the embedded pulse sequence in Fig. 6(b) that the pulse sequence does not fluctuate. The background is clear and there are no random and chaotic noise pulses, which proves that the DSML state is stable[42-43]. The interval between adjacent pulses is 142.6 ns corresponding to the operating period of the mode-locked pulse and the fundamental frequency of 7 MHz in the cavity.

To further demonstrate the stability of DSML state at the room temperature, the spectrum data is collected every 10 minutes in an hour. The experimental results are shown in Fig. 7. Fig. 7(a) shows the overall distributionof the seven spectrum remaining consistent shapes. The result shows that the spectrum distribution is basically same, indicating that the DSML state is stable. Fig. 7(b) is the quantitative analysis of the fluctuation of the spectrum wavelength. The results show that there is no change in the center wavelength and the spectrum bandwidth has a change less than 0.1 nm, which indicates that the spectrum stability is good. The FWHM of the optical spectrum varies slightly between 29.14 nm and 29.20 nm, which may be due to the error in the measurement of the experimental instrument.

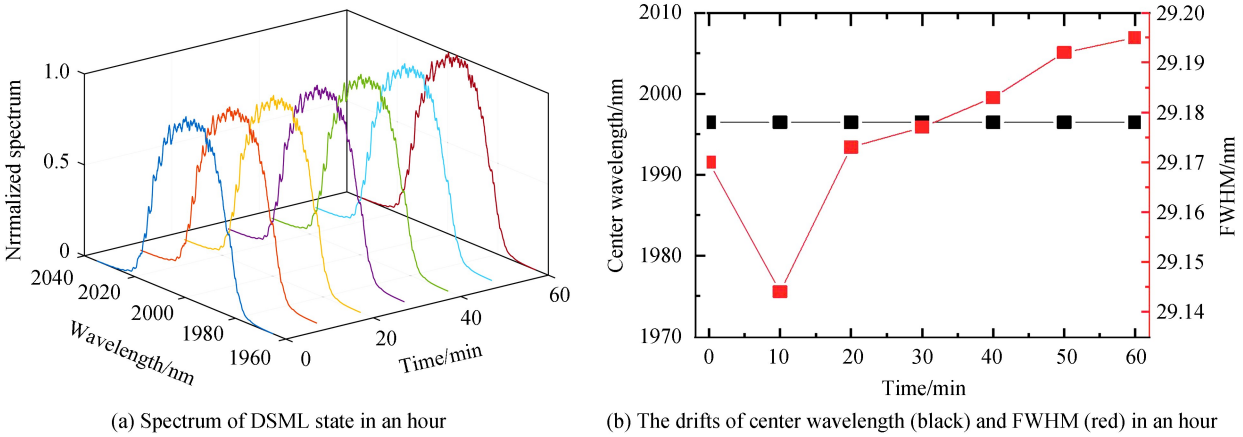

(a) Spectrum of DSML state in an hour

(b) The drifts of center wavelength (black) and FWHM (red) in an hour

Fig.7 Stability of TDFL operating at DSML state in an hour

2.3 Switching between MW state and DSML state

Fig. 8 shows the switching between MW state and DSML state of the TDFL at four different PC states

at the same pump power of 8.0 W. The function of saturable absorber and amplitude equalizer of NALM can be switched with the shift value of θ by adjusting the PC. As the result the switching between MW state and DSML state can be achieved. It can be clearly seen that first spectrum (blue) and second spectrum (red) are MW state, in this case, NALM is used as an amplitude equalizer. Third spectrum (yellow) and fourth spectrum (purple) are DSML state, in this case, NALM acts as a saturable absorber. And third spectrum (yellow) has a significant modulation phenomenon which can be attributed to the combined effects of the Lyot filtering effect, loss and gain of the laser cavity[40]. The transmittance of the Lyot filter in this experimental device can be expressed by the following formula[21]

$$T=1-\sin^2\left(\frac{\Delta n\pi L}{\lambda}\right)\sin^2(2\beta) \tag{3}$$

where T is the transmittance of the filter, Δn is the birefringence parameter of PMF, L is the length of PMF, and λ is the wavelength. The appropriate value of β can be obtained by carefully adjusting the state of PC. The transmittance of the Lyot filter is shown as Fig. 9.

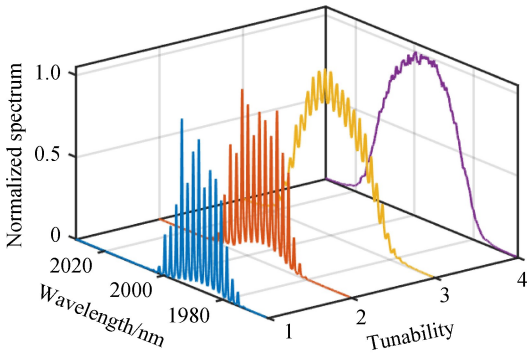

Fig.8 Switching between MW state and DSML state by adjusting the PC

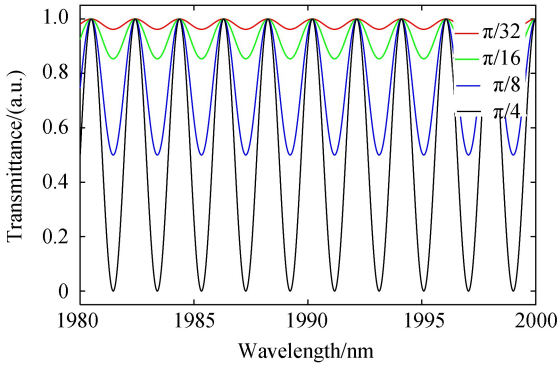

Fig.9 Transmission spectrum of Lyot filter

According to Fig.9, β is taken four different values of π/32, π/16, π/8, and π/4, respectively. When the value of β is relatively big, the extinction of the Lyot filter is relatively high, that is, the modulation depth of Lyot is higher[40]. In this case, the laser experiences different losses at different wavelengths when propagating in the PMF, and the gain bandwidth filtering effect is not obvious compared with the optical fiber birefringence filtering effect[21]. Correspondingly, when the value of β is gradually reduced by adjusting PC, the extinction ratio of the Lyot filter is gradually reduced, the modulation depth of the Lyot filter is weakened, and the laser propagating in the PMF has a small loss at different wavelengths. At this time, the gain bandwidth filtering effect is stronger than that of the PMF[21]. The significant modulation phenomenon of third spectrum (yellow) shows that although the effect of fiber birefringence filtering is not obvious in this case and it does not completely disappear.

3 Conclusion

In summary, based on the combination of NALM and Lyot filter, we achieve a state-switchable thulium-doped fiber laser. By adjusting the PC and the pump power, two different operating states are obtained: MW and DSML. At the pump power between 3.7 W and 7.0 W, TDFL can operate at MW state with 8 wavelength peaks and the peak-to-peak filtering bandwidth about 1.94 nm. With the pump power of 7.0 W to 10.5 W, the TDFL can operate stably at DSML state with highly energy pulse of 49 nJ at the repetition rate of 7 MHz. By adjusting PC, the switching between MW and DSML is realized, and the reason for the switching also has been explained.

References

[1] SUN Biao, LUO Jia-qi, YAN Zhi-yu, *et al*. 1867-2010 nm tunable femtosecond thulium-doped all-fiber laser[J]. *Optics Express*, 2017, **25**(8): 8997-9002.

[2] MA Wan-zhuo, WANG Tian-shu, WANG Fu-ren, *et al*. 2.07μm, 10 GHz repetition rate, multi-wavelength actively mode-locked fiber laser[J]. *IEEE Photonics Technology Letters*, 2019, **31**(3): 242-245.

[3] WANG Ya-zhou, LI Jian-feng, ZHAI Bo, *et al*. Tunable and switchable dual-wavelength mode-locked Tm^{3+}-doped fiber laser based on a fiber taper[J]. *Optics Express*, 2016, **24**(14): 15299-15306.

[4] WANG Ya-zhou, LI Jian-feng, HONG Lu-jun, *et al*. Coexistence of dissipative soliton and stretched pulse in dual-wavelength mode-locked Tm-doped fiber laser with strong third-order dispersion[J]. *Optics Express*, 2018, **26**(14): 18190-18201.

[5] GRZES P, SWIDERSKI J. Gain-switched 2-μm fiber laser system providing kilowatt peak-power mode-locked resembling pulses and its application tosupercontinuum generation in fluoride fibers[J]. *IEEE Photonics Journal*, 2018, **10**(1): 1500408.

[6] WANG Meng, HUANG Yi-jian, YU Li, *et al*. Multi-wavelength thulium-doped fiber laser using a micro fiber-optic Fabry-Perot interferometer[J]. *IEEE Photonics Journal*, 2018, **10**(4): 1502808.

[7] LIU Xue-song, ZHAN Li, LUO Shou-yu, *et al*. Multiwavelength erbium-doped fiber laser based on a nonlinear amplifying loop mirror assisted by un-pumped EDF[J]. *Optics Express*, 2012, **20**(7): 7088-7094.

[8] LIU Shou, YAN Feng-ping, FENG Ting, *et al*. Switchable and spacing-tunable dual-wavelength thulium-doped silica fiber laser based on a nonlinear amplifier loop mirror[J]. *Applied Optics*, 2014, **53**(24): 5522-5526.

[9] LIU Xue-song, ZHAN Li, LIU Jin-mei, *et al*. Dual-state multiwavelength fiber laser: nanosecond pulses and tunable continuous waves[J]. *IEEE Photonics Technology Letters*, 2013, **25**(17): 1737-1740.

[10] GUTIERREZ-GUTIERREZ J, ROJAS-LAGUNA R, ESTUDILLO-AYALA J M, *et al*. Switchable and multi-wavelength linear fiber laser based on Fabry - Perot and Mach - Zehnder interferometers[J]. *Optics Communications*, 2016, **374**: 39-44.

[11] LATIFF A A, SHAMSUDIN H, TIU Z C, *et al*. Switchable soliton mode-locked and multi-wavelength operation in thulium-doped all-fiber ring laser[J]. *Journal of Nonlinear Optical Physics and Materials*, 2016, **25**(3): 1650034.

[12] LIU Shuo, YAN Feng-ping, TING Feng, *et al*. Multi-wavelength thulium-doped fiber laser using a fiber-based lyot filter[J]. *IEEE Photonics Technology Letters*, 2016, **28**(8): 864-867.

[13] PENG Wan-jing, YAN Feng-ping, LI Qi, *et al*. A 1.97 μm multiwavelength thulium-doped silica fiber laser based on a nonlinear amplifier loop mirror[J]. *Laser Physics Letters*, 2013, **10**: 115102.

[14] AHMAD H, SHARBIRIN A S, SAMION M Z, *et al*. All-fiber multimode interferometer for the generation of a switchable multi-wavelength thulium-doped fiber laser[J]. *Applied Optics*, 2017, **56**(21): 5865-5870.

[15] YAN Zhi-yu, TANG Yu-long, SUN Biao, *et al*. Switchable multi-wavelength Tm-doped mode-locked fiber laser[J]. *Optics Letters*, 2015, **40**(9): 1916-1919.

[16] AHMAD H, AHMED M H M, SAMION M Z, *et al*. All fiber multiwavelength Tm-doped double-clad fiber laser assisted by four-wave mixing in highly nonlinear fiber and Sagnac loop mirror[J]. *Optics Communications*, 2020, **456**: 124589.

[17] YIN Tao-ce, MAO Barerem-melgueba, WEI Yi-zhen, *et al*. Widely wavelength-tunable 2 μm Brillouin fiber laser incorporating a highly germania-doped fiber[J]. *Applied Optics*, 2018, **57**(23): 6831-6834.

[18] JIN Xiao-xi, WANG Xiong, WANG Xiao-lin, *et al*. Tunable multiwavelength mode-locked Tm/Ho-doped fiber laser based on a nonlinear amplified loop mirror[J]. *Applied Optics*, 2015, **54**(28): 8260-8264.

[19] CHEN He, CHEN Sheng-ping, JIANG Zong-fu, *et al*. 80 nJ ultrafast dissipative soliton generation in dumbbell-shaped mode-locked fiber laser[J]. *Optics Letters*, 2016, **41**(18): 4210-4213.

[20] CHENG Zhao-cheng, LI Hui-hui, WANG Pu, *et al*. Simulation of generation of dissipative soliton, dissipative soliton resonance and noise-like pulse in Yb-doped mode-locked fiber lasers[J]. *Optics Express*, 2015, **23**(5): 5972-5981.

[21] YUN Ling. Generation of vector dissipative and conventional solitons in large normal dispersion regime[J]. *Optics Express*, 2017, **25**(16): 18751-18759.

[22] WANG Yu, ALAM S U, OBRAZTSOVA E D, *et al*. Generation of stretched pulses and dissipative solitons at 2 μm from an all-fiber mode-locked laser using carbon nanotube saturable absorbers[J]. *Optics Letters*, 2016, **41**(16): 3864-3867.

[23] OKTEM B, ÜLGÜDÜR C, LLDAY F. Soliton-similariton fibre laser[J]. *Nature Photonics*, 2010, **4**(5): 307-311.

[24] WANG Pan, HU Da-ke, ZHAO Li-ying, *et al*. Dissipative rogue waves among noise-like pulses in a Tm fiber laser mode locked by a monolayer MoS2 saturable absorber[J]. *IEEE Journal on Selected Topics in Quantum Electronics*, 2018, **24**(3): 1800207.

[25] WANG Xiao-fa, XIA Qing, GU Bin. A 1.9 μm noise-like mode-locked fiber laser based on compact figure-9 resonator [J]. *Optics Communications*, 2019, **434**: 180-183.

[26] CAI Jun-hao, CHEN He, CHEN Sheng-ping, *et al*. Compressibility of dissipative solitons in mode-locked all-normal-dispersion fiber lasers[J]. *Journal of Lightwave Technology*, 2018, **36**(11): 2142-2151.

[27] AKHMEDIEV N, SOTO-CRESPO J M, PETER Vouzas, *et al*. Dissipative solitons with extreme spikes in the normal and anomalous dispersion regimes[J]. *Philosophical Transactions of The Royal Society A Mathematical Physical and Engineering Sciences*, 2018, **376**(2124): 20180023.

[28] GAPONOV D A, DAULIAT R, DARWICH D, *et al*. High-power passively mode-locked dissipative soliton fiber laser featuring cladding-pumped non-CVD thulium-doped fiber[J]. *Journal of the Optical Society of America B*, 2015, **32**

(8): 1656-1659.

[29] HAN Dong-dong, YUN Ling. Q-switched mode-locking and dissipative soliton operations in a large-anomalous-dispersion fiber laser[J].*Optical Engineering*, 2012, **51**(4): 044201.

[30] WANG Lei-ran, LIU Xue-ming, GONG Yong-kang. Experimental research on high-energy dissipative solitons in an erbium-doped fiber laser[J].*Acta Physica Sinica*, 2010, **59**(9): 6200-6204.

[31] LI Nan-xi, XUE Jin, OUYANG Chun-mei,*et al*. Cavity-length optimization for high energy pulse generation in a long cavity passively mode-locked all-fiber ring laser[J]. *Applied Optics*, 2012, **51**(17): 3726-3730.

[32] ZHOU Jia-qi, GU Xi-jia. 32-nJ 615-fs stable dissipative soliton ring cavity fiber laser with raman scattering[J].*IEEE Photonics Technology Letters*, 2016, **28**(4): 453-456.

[33] AGUERGARAY C, BRODERICK N G R, ERKINTALO M,*et al*. Mode-locked femtosecond all-normal all-PM Yb-doped fiber laser using a nonlinear amplifying loop mirror[J]. *Optics Express*, 2012, **20**(10): 10545-10551.

[34] ERKINTALO M, AGUERGARAY C, RUNGE A,*et al*. Environmentally stable all-PM all-fiber giant chirp oscillator [J]. *Optics Express*, 2012, **20**(20): 22669-22674.

[35] WANG Si-ming, FAN Xu-liang, ZHAO Lu-ming,*et al*. Dissipative vector soliton in a dispersion-managed fiber laser with normal dispersion[J]. *Applied Optics*, 2014, **53**(35): 8216-8221.

[36] YANG Nan, HUANG Chong-yuan, TANG Yu-long,*et al*. 12 nJ 2 μm dissipative soliton fiber laser[J]. *Laser Physics Letters*, 2015, **12**(5): 055101.

[37] DU Juan, WANG Qing-kai, JIANG Guo-bao, *et al*. Ytterbium-doped fiber laser passively mode locked by few-layer Molybdenum Disulfide (MoS2) saturable absorber functioned with evanescent field interaction[J]. *Scientific Reports*, 2014, **4**: 6346.

[38] ZHAO Jun-qing, LI Lei, ZHAO Lu-ming,*et al*. Cavity-birefringence-dependent h-shaped pulse generation in a thulium-holmium-doped fiber laser[J]. *Optics Letters*, 2018, **43**(2): 247-250.

[39] WANG Xiao-fa, PENG Xiao-ling, ZHANG Jun-hong. Multistate passively mode-locked thulium-doped fiber laser with nonlinear amplifying loop mirror[J].*Applied Optics*, 2018, **57**(13): 3410-3414.

[40] LUO Xing, TUAN Tong-hoang, SAINI Than-singh,*et al*. Tunable and switchable all-fiber dual-wavelength mode locked laser based on Lyot filtering effect[J]. *Optics Express*, 2019, **27**(10): 14635-14647.

[41] ZHAO Jun-qing, LI Lei, ZHAO Lu-ming,*et al*. Tunable and switchable harmonic h-shaped pulse generation in a 3.03 km ultralong mode-locked thulium-doped fiber laser[J]. *Photonics Research*, 2019, **7**(3): 332-340.

[42] LAU K Y, BAKAR Abu M H, MUHAMMAD F D, *et al*. Dual-wavelength, mode-locked erbium-doped fiber laser employing a graphene/polymethyl-methacrylate saturable absorber[J]. *Optics Express*, 2018, **26**(10): 12790-12800.

[43] LUO Ai-ping, ZHENG Xu-wu, LIU Meng, *et al*. Generation of a noiselike soliton molecule induced by a comb filter in a figure-eight fiber laser[J]. *Applied Physics Express B*, 2015, **8**(4): 042702.